ASSYMMETRY OF TIDE AND SUSPENDED SEDIMENT CONCENTRATIONS OBSERVED AT THE NORTH-EASTERN PART OF THE MEGHNA ESTUARY

Mohammad Asad Hussain[1], Yoshimitsu Tajima[2], Mohammed Abed Hossain[3] and Sohel Rana[4]

Field investigations have been conducted at the north-eastern part of the Meghna Estuary to collect tidal water level, velocity and turbidity. It is found that strong vertical as well as horizontal tidal asymmetry exists around the highly accreting Urir Char Island of the Meghna Estuary. Along the northern channel of Urir Char Island flood velocity exceeds ebb velocity which would induce residual transport of coarse sediments towards land. Also duration of slack water duration before flood is much longer than that before ebb indicating residual transport of fine sediments. The phase lag between peak flood velocity and peak turbidity during the flood duration is about two hours, while it is less than one hour between peak ebb velocity and peak turbidity during ebb duration. A 'second peak' in the turbidity profiles is observed which appears to be caused by rundown of ebb tidal flow from the shallow intertidal mudflats around the Urir Char Island. A 2DH numerical model based on non-linear shallow water equations have been employed to explain the observation data. From the simulation results, it is evident that the horizontal advection pattern plays significant role in residual transport of suspended sediments.

Keywords: tidal asymmetry, Meghna Estuary, numerical model

INTRODUCTION

The Meghna Estuary (Fig. 1) of Bangladesh discharges the combined flow of three major river systems of the world: The Ganges, The Brahmaputra and The Meghna River. Sediment discharge through the Meghna Estuary is the highest (Coleman, 1969) and water discharge is the third highest in the world, only after Amazon and Congo Rivers (Milliman, 1991). The estuary is located at the northern part of the Bay of Bengal and experiences large tidal fluctuations of up to more than 6 m at some locations (de Wilde, 2011). Constant processes of erosion and accretion are observed in the Meghna Estuary under the complex interactions among large river discharge, enormous sediment load, strong tidal forces and estuarine circulations. Based on the satellite images, from 1973 to 2000 the erosion and accretion in the estuary has been estimated as 863.66 sq.km. and 1371.68 sq.km., respectively. This gives a net accretion of 508.02 sq.km. at a rate of 18.8 sq.km. per year. From 2000 to 2008 the rate has increased to 25 sq.km. per year. Such high rate of coastline movement cannot be found at any other parts of the world (de Wilde 2011). While estuarine morphological changes strongly depend on various physical factors such as: water and sediment discharge through the river, wind, waves and tides, in case of Meghna Estuary tide induced residual current dominantly determines the sedimentation process (Azam *et al.,* 2000). At the same time, tidal current itself is also highly influenced by dynamic morphological changes. So, it is essential to investigate the tidal characteristics of the Meghna Estuary to understand the erosion-accretion processes in the estuary.

Tidal asymmetry is one of the most important factors which cause residual sediment transport in estuaries (Dronkers, 1986 and Wang *et al.*, 1999). Usually 'tidal asymmetry' refers to the distortion of tidal waves which makes the flood period unequal to the ebb period. Tide is called 'flood dominant' when the period of water level rise is shorter than the period of water level fall and it is called 'ebb dominant' when the opposite happens. While analyzing the residual sediment transport characteristics of the Western Scheldt estuary in the Netherlands, Wang *et al.* (1999) made a distinction between 'horizontal tide' and 'vertical tide' in order to relate tidal asymmetry with morphological development via residual sediment transport. The authors adopted the definition of vertical tidal asymmetry as the inequality between flood and ebb periods in terms of water level variations. The horizontal tide refers to tidal flow velocity and it is considered asymmetric if it generates residual sediment transport. The horizontal tidal asymmetry again has been divided into two types: asymmetry between maximum flood and ebb velocity and asymmetry between flood and ebb slack water durations. If the maximum flood velocity exceeds the maximum ebb velocity it is termed as flood dominant and vice versa. This type of asymmetry, when flood dominant, tends to induce residual bed load and suspended load transport of coarse sediments in flood direction, as the sediment transport non-linearly responds to velocity. On the other hand, a situation when the duration of slack water before ebb (SBE) exceeds the slack water

[1] Department of Civil Engineering, University of Tokyo, 7-3-1 Hongo, Bunkyo-ku, Tokyo 113-8656, Japan
[2] Department of Civil Engineering, University of Tokyo, 7-3-1 Hongo, Bunkyo-ku, Tokyo 113-8656, Japan
[3] Institute of Water and Flood Management, Bangladesh Univ. of Engineering. and Tech., Dhaka 1000, Bangladesh
[4] GIS Unit, Local Government Engineering Department, Agargaon, Shere Bangla Nagar, Dhaka 1207, Bangladesh

before flood (SBF) is termed as flood dominant and vice versa. This type of asymmetry, when flood dominant, will favor a residual sediment transport of fine sediments in the flood direction. Based on theoretical considerations and filed observations, Dronkers (1986) also showed that the asymmetry of the flood and ebb limbs of the tidal velocity curve, and in particular the length of the high water slack period as compared to the low water slack, controls the net sediment budget in an estuary. The present paper focuses on the asymmetry of tide and resulting suspended sediment concentrations observed along the northern channel of Urir Char Island located at the north-eastern part of Meghna Estuary.

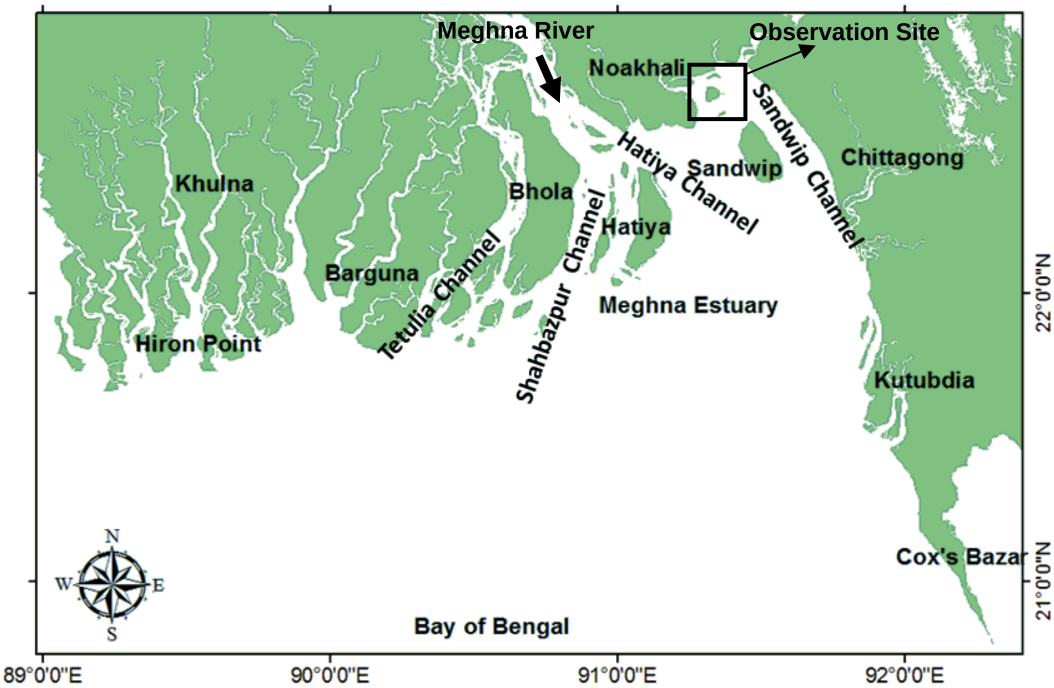

Figure 1. Meghna Estuary and area of observation sites

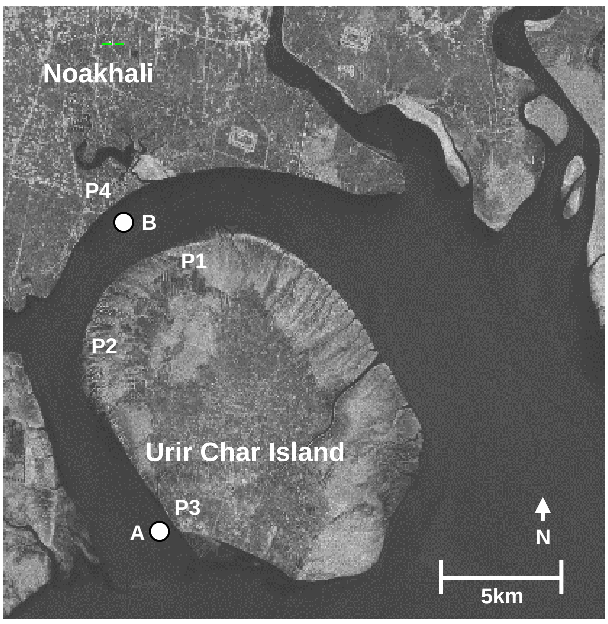

Figure 2. Observation sites around Urir Char Island

DATA AND METHODOLOGY

Measured data in the Meghna Estuary is scarce especially during the monsoon season due to difficulties like: inaccessibility to the site, stormy conditions as well as unavailability of measurement vessels. This causes a major difficulty against in-depth investigation of erosion-accretion processes in the study area. During the present study, field investigations were conducted both during winter and monsoon seasons to collect hydrodynamic data in the Meghna Estuary at the observation sites A and B shown in Fig.2.

On site observations of TWL (at location A and B of Fig. 2), tidal velocity (at location B) and turbidity (at location B) were made along the northern and western channels of Urir Char Island. Simultaneous measurements of TWLs were made at locations A and B during the month of December in 2012, which is winter season in the study area. On the other hand, during July of 2013, which is monsoon season in the study area, measurements of TWL, tidal velocity and turbidity were made at location B. The study area is characterized by distinct meteorological as well as hydrodynamic conditions during the monsoon and winter seasons; as during monsoon there is strong south wind (11.5-28.0 m/s), large amount of precipitations in the upper catchments resulting huge river water and sediment discharge through the river mouth and during winter there is relatively calm north wind with very small river water and sediment discharge through the Meghna Estuary (Islam *et al.*, 2002).

A two-dimensional depth-averaged hydrodynamic model based on non-linear shallow water equations has been applied to investigate the spatial distribution of tidal flow features in the study area. The model is discretized based on a spherical coordinate system and it accounts for Coriolis Effect for computations of large-scale tidal currents. Bathymetry of the Meghna Estuary is obtained from the GEBCO (General Bathymetric Chart of the Oceans) 30arc-second free source data. The GEBCO data has reasonably good resolution and also it can be considered as relatively new because the measured bathymetry data in the Meghna Estuary dates back 1997. Also, as already mentioned Meghna Estuary is very dynamic where coastlines change quite frequently. So the coastline inaccuracies of GEBCO data are first rectified with the help of ALOS-PALSAR (Advanced Land Observing Satellite's Phased Array L-band Synthetic Aperture Radar) satellite images. The most dynamic parts of the Meghna Estuary, from Hatiya Channel at the western end to the Sandwip Channel at the eastern, are covered by these satellite images. The PALSAR image acquired during April 2011, has been employed to obtain the present coastlines of the Meghna Estuary area. The grid size for the numerical model is thirty second (about 926m) with 150 grid points along the north-south direction and 250 grid points along east-west which gives a domain size of 138.9km by 231.5km. Bathymetry of the Meghna Estuary where coastlines are updated by satellite images and unrealistic nearshore water depths are corrected by bathymetric survey at selected locations is shown in Fig. 3.

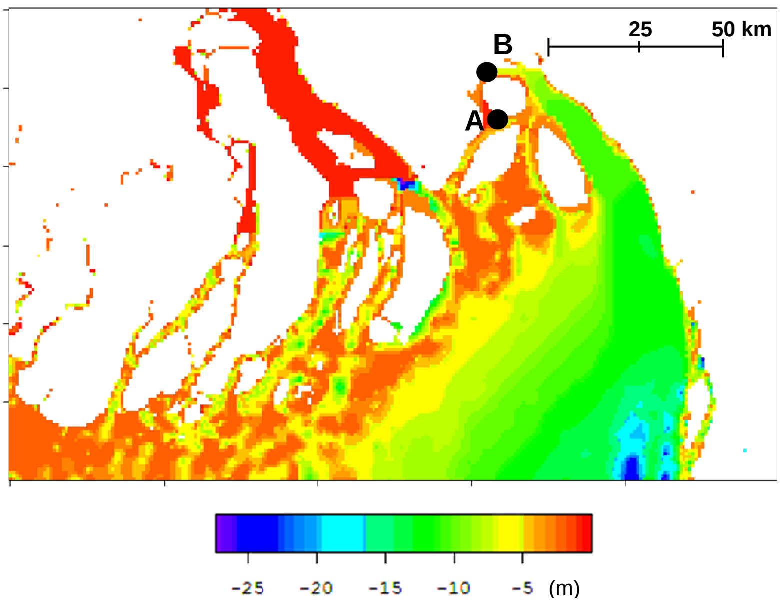

Figure 3. Bathymetry of the Meghna Estuary after correcting unrealistic water depth of GEBCO data and updating the coastlines using satellite images.

The tidal water levels at the southern boundary along each grid point are obtained by applying Naotide (Matsumoto, 2000), a global ocean tide model. From the computed TWLs of Naotide it can be observed that tidal phase at the western part of the computation domain leads the tidal phase at the eastern part by two hours (Hussain *et al.*, 2013) which is also in agreement with the findings of de Wilde (2012). Also, tidal range along the eastern part of the computation domain is 0.5m larger than that along the western part during the spring tide periods. While tidal ranges are almost the same at both eastern and western parts during the neap periods.

The 2DH model is then calibrated with the TWL data obtained during December 2012 and validated with observed TWL and velocity data obtained during July 2013 with reasonably good accuracy (Hussain and Tajima, 2014). Finally physical mechanisms of the observed tidal velocity and fluctuations of turbidity data during a tidal cycle are discussed with the aid of the numerical model results.

RESULTS AND DISCUSSION

Topographic Features

The target area of the present research is characterized by large intertidal mudflats which are surrounding major parts of the offshore islands. It has been found from satellite image analyses that Urir Char Island has been accreting along its northern, western and eastern parts where the island is surrounded by large mudflats. While, the island is eroding along the southern part which is devoid of mudflats (Hussain *et al.*, 2014). Photographs taken during the field investigation at different locations (shown in Fig 2.) in the study area are shown in Fig 4. Photographs P1 and P2 in Fig. 4 show the large extent of intertidal mudflats along the northern and north-western parts of the Urir Char Island, respectively.

Figure 4. Topographic features around the observation site; P1 and P2: mudflats along the northern and north-western part, P3: relatively steep slope bank at the south-west part of Urir Char Island and P4: very steep slope erosion prone coast at Noakhali main land (locations are shown in Fig.2)

There is relatively steep slope with signs of erosion at the southwest part of Urir Char, as shown in photograph P3 in the same Figure. During the field visit, it was observed that the mainland at the northern part of the Urir Char Island, Noakhali, had a very steep slope along the coastline (P4 in same Figure) and was eroding at a severe rate during the monsoon of 2013. It was also observed that the bathymetry along the channel at the western part of Urir Char Island (to the left of P2 shown in Fig. 2) was very shallow and the channel could not be crossed using a country boat during the ebb tide periods. The water quality conditions at the study site suggested that turbidity is directly related to suspended sediment concentrations, as no other factor appeared dominant to influence turbidity at the site.

Tidal Water Level, Tidal Velocity and Turbidity

Fig. 5 shows the observed TWLs at locations A (blue line) and B (red line) simultaneously measured during December 2012. At location A, during ebb tide, tidal water level reached below the level of the pressure sensor resulting in no tidal water level variation for a short duration. From this Figure it is clearly evident that at both locations TWLs show a forward leaning profile with short rising period and a long falling period. At location B, north of Urir Char Island, the tidal range is about a meter higher than that at location A, south of Urir Char Island, during the measurement period. From the tidal profiles it is also evident that tidal asymmetry is relatively higher at the northern part of the Urir Char Island than that at the south of the island.

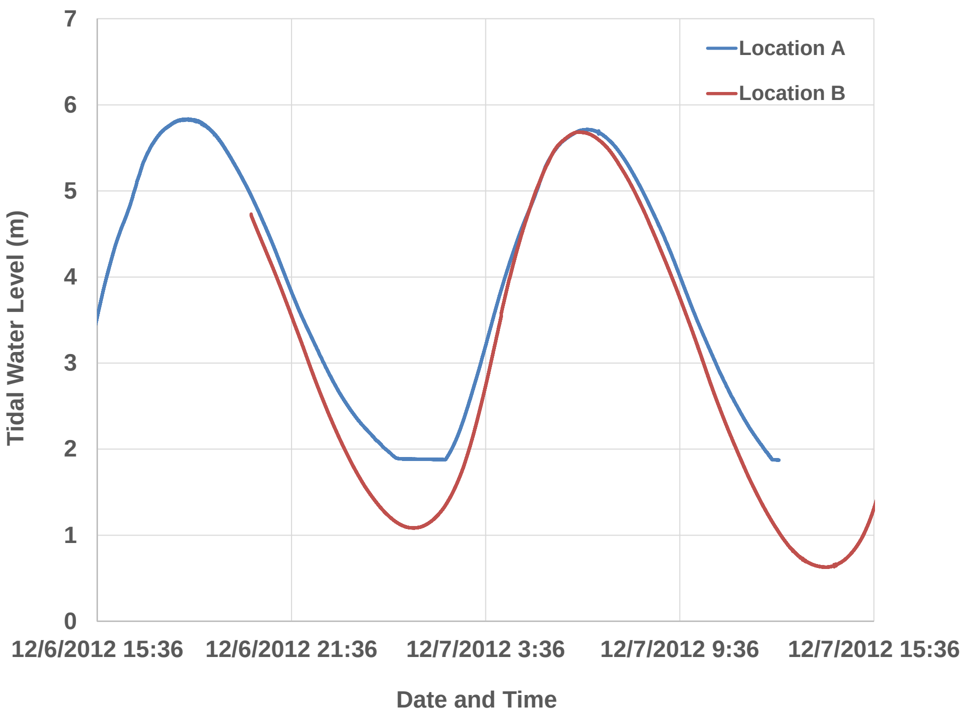

Figure 5. TWL at locations A and B of Fig. 2 simultaneously measured during December 2012

Fig. 6 shows the observed tidal water level (black line) along with the horizontal velocity components (red line: northward and blue line: eastward) and turbidity (dotted line) during a tidal cycle measured at location B during July 2013, monsoon season in the study area. The tidal water level clearly shows a forward leaning profile with a shorter period of water level rise and prolonged duration of water level fall. So, along the northern channel of Urir Char Island, there exists vertical flood dominance of tidal asymmetry. It can also be noticed that flood velocity is towards south-west direction at the measurement location. This indicates that primarily tidal water enters the measurement location from the eastern side through the Sandwip Channel as there is very shallow water areas along the western channel of Urir Char Island. The magnitude of flood velocity is also significantly higher than the ebb velocity. This suggests existence of horizontal flood dominance along the channel and it will induce a residual bed load and suspended load transport of coarse sediments to the flood direction (Dronkers, 1986 and Wang et.al., 1999) i.e. southwestward direction. Again, during the flood period larger velocity is observed towards west direction compared to south. While during the ebb period larger velocity is observed towards north direction compared to east. We have discussed this phenomena through the aid of numerical simulation later in this paper. It is also seen from the figure that the duration of Slack tide Before Ebb (SBE) is significantly shorter than the duration of Slack tide Before Flood (SBF). This favors the residual transport of fine suspended sediments in the ebb direction (Wang, 1999).

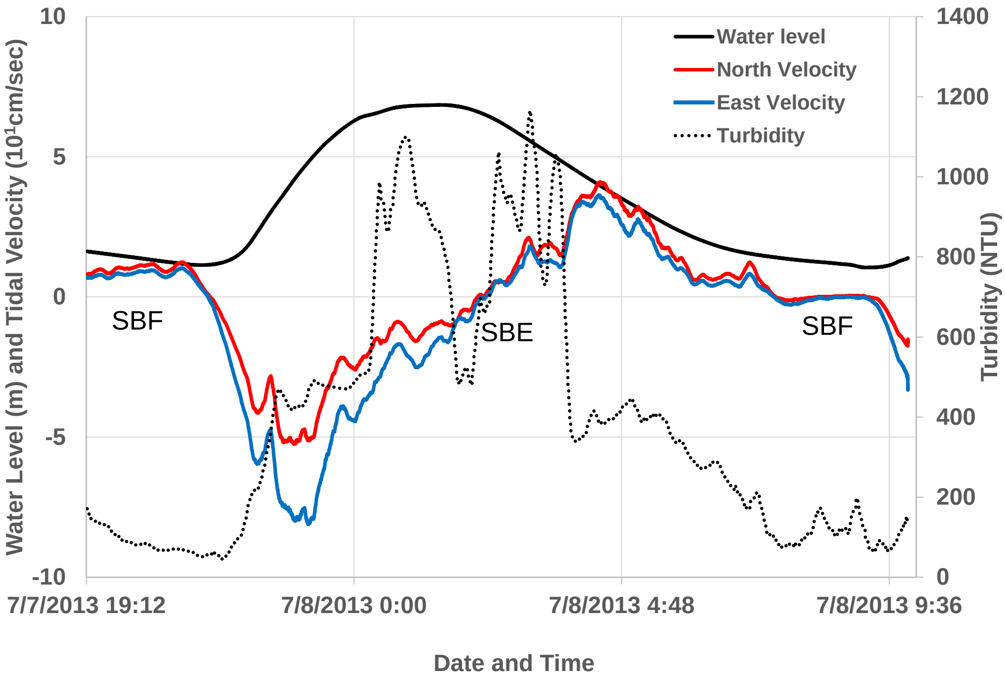

Notably, from the turbidity distribution of Fig. 6 two peaks are observed on either side of the SBE. From the figure it is evident that peaks of flood velocity and turbidity have clear phase lag of about two hours. While the increase of velocity also increases local pick up rate of suspended sediments, it should take certain time to increase suspended sediment concentration. This phase lag may also be partially due to horizontal advections of suspended sediments. Flood tide flows toward shallower water depth and thus the incoming flow velocity tends to be slower than the outgoing velocity and this feature also affects to slow down the increase of suspended sediment concentration. During the SBE there is sharp fall of turbidity values (less suspended sediments) but as soon as the ebb velocity appears there is another peak of similar magnitude. In other words, during ebb tide the peak of the suspended sediments occurs before the peak ebb velocity. This might also be due to horizontal advection patterns of suspended sediment. The appearance of the 'second peak' in the turbidity curve has been further explained in the later part of this paper. Finally, when the peak of the ebb current appears a small rise is observed in the turbidity values due to the smaller magnitude of ebb current. It is interesting to note that the phase lag between peaks of ebb tide velocity and following peak turbidity is less than one hour, which is much shorter than that during the flood tide.

Tidal Current Simulations

As already mentioned a 2DH hydrodynamic model based on non-linear shallow water equations has been applied to explain the spatial distribution of tidal currents around the Urir Char Island of Meghna Estuary. The computations are done from July 1 to 10, 2013 to obtain the tidal flow field during the time of field measurement. The calculated input TWLs along the southern boundary of the computation domain from Naotide shows that there was spring tide periods during the field measurement.

Fig. 7 shows the simulated spatial velocity distributions along with velocity magnitude in contours during the peak flood velocity at the measurement location B. The lighter color in the contour map indicates higher magnitude of velocity. It is clearly evident from this figure that at the measurement site tidal water enters primarily through the eastern side from the Sandwip Channel because the areas along the western channel of Urir Char is very shallow. A tidal meeting point appears at the western part of Urir Char Island where tidal currents from the south meets the same from the north. The area is also marked by dark contours as the magnitude of tidal velocity is smallest at this location. The fact that the peak in the turbidity values of Fig. 6 appears with a two hour phase lag after the peak of flood velocity may be explained from this spatial velocity distribution. Understandably, the large tidal current will cause quicker pickup of local sediments at the measurement location B. The small tidal currents along the western channel of Urir Char Island in-combination with the strong currents all along the northern channel, as can be seen from Fig. 7, will continue to supply sediments from the eastern side towards location B and create a peak in the turbidity values with such a long phase lag. Such kind of phenomena was also observed by Barua (1990) at the east Hatuya channel of Meghna Estuary. From Fig. 7 it is also evident that due to the coastline configurations flood water is directed towards south-west with a larger component in the western direction. This is why larger velocity was observed towards west compared to south during the flood period in Fig. 6. From the velocity field of Fig.7, other than the northern and north-eastern parts of the Urir Char Island high velocity magnitude is also observed at the southern part of the island. It appears that the large volume of incoming tide from the Sandwip Channel is distributed towards the northern part of Urir Char Island as well as along the southern channel. Tidal currents also converge towards the south of Urir Char Island from the other two southern channels during the flood period.

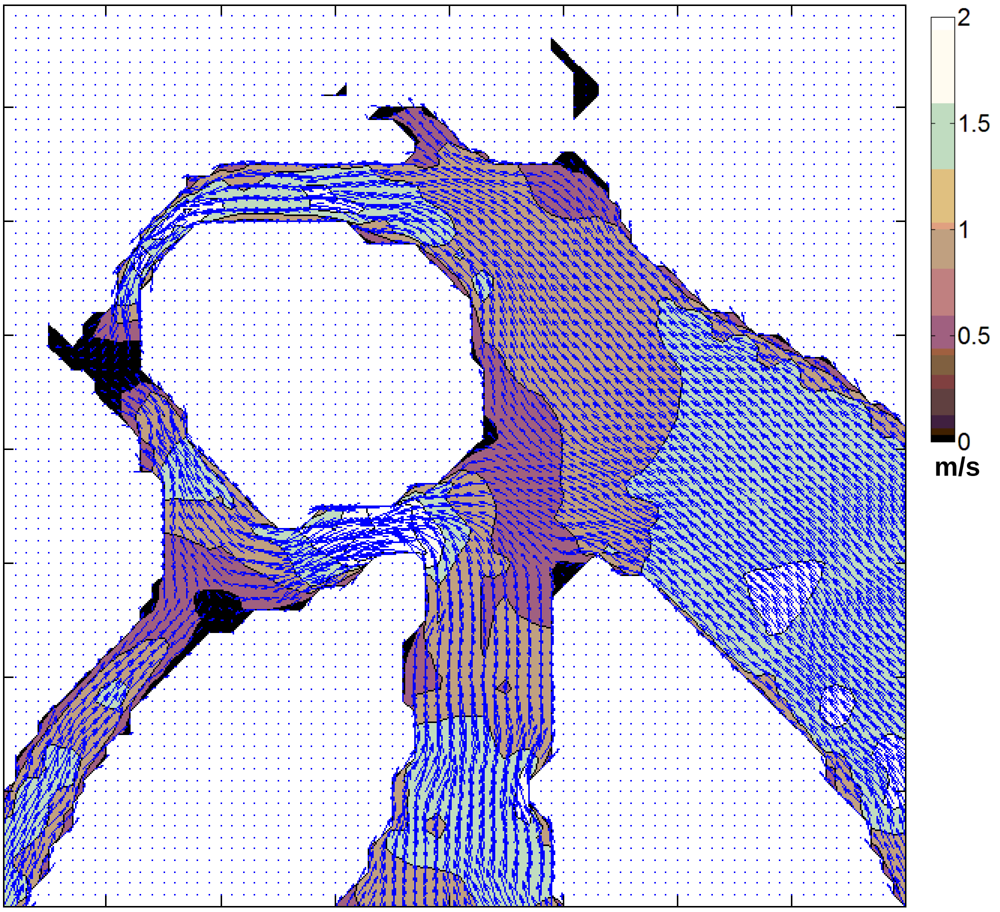

Figure 7. Simulated tidal velocity distribution during peak flood velocity at the measurement location B, contour shows velocity magnitude in m/s

Simulated tidal velocity distribution results during the slack water period before ebb (SBE) at measurement location B is shown in Fig. 8. Dark patches in Fig. 8 show very small tidal velocity around the measurement location B during SBE. The slack water along the northern channel causes the sharp fall of turbidity values in Fig. 6 and at the same time it may enhance the ‘second peak’ in the observed turbidity profile. The rundown of tidal water from the intertidal mudflats appears to cause this peak. As the tidal water starts to recede from the intertidal mudflats with high amount of sediments in suspension, it suddenly increases the sediment concentration (turbidity value in the Fig. 6) along the channel where suspended sediments were very small during the time of SBE due to small flow velocity. The turbidity value of the ‘second peak’ also shows a sudden fall because the suspended sediment concentration sharply reduces when the supply of sediments are cutoff when the mudflats are exposed. The small dunes created by the waves during the ebb period all along the mudflats, as can be seen in Fig. 4 (P1 and P2) act as a boundary to prevent the sediment supply towards the main channels as soon as the mudflats gets exposed during the ebb period. From Fig. 8 it also evident that ebb velocity along the two southern channels is relatively higher compared to the ebb velocity along Sandwip Channel. It appears that some part of the tidal water which approaches from the Sandwip Channel recedes through the two southern channels, resulting larger ebb flow through these channels.

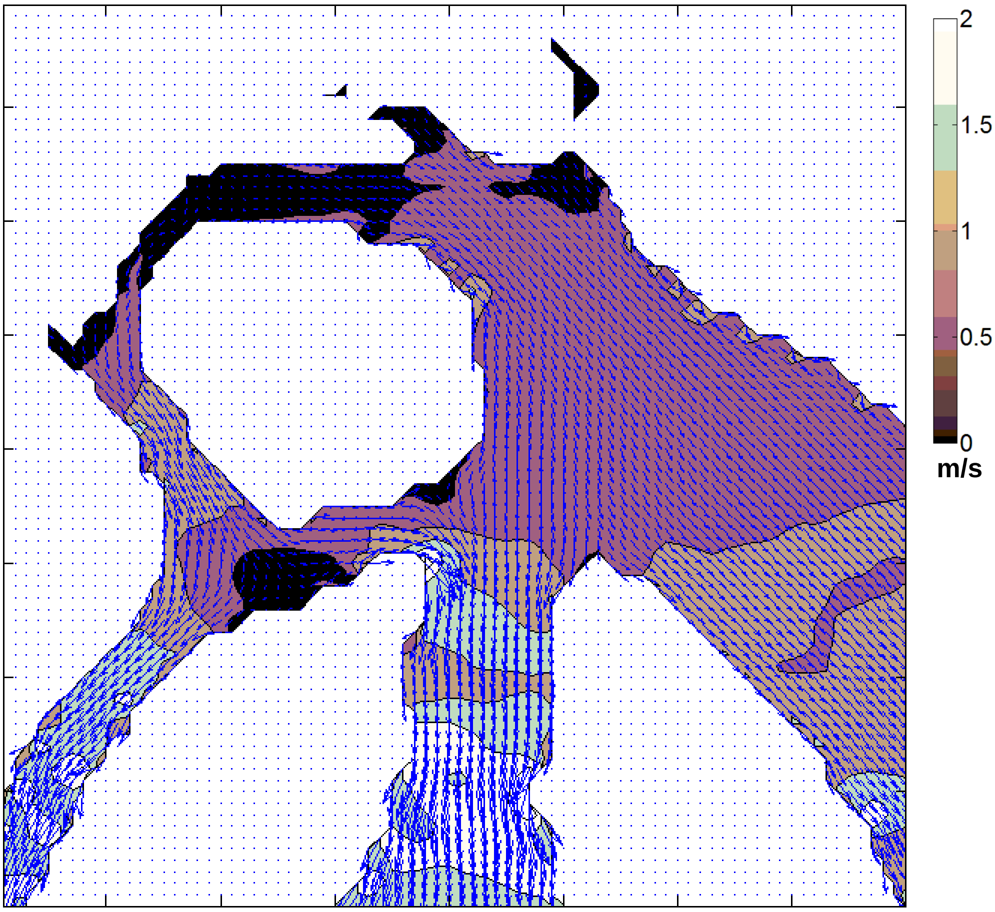

Figure 8. Simulated tidal velocity distribution during slack before ebb (SBE) at the measurement location B, along with contour of velocity magnitude (m/s)

Fig. 9 shows the spatial distribution of tidal velocity around the study area when the ebb velocity is highest at the measurement location B. It is evident from this Figure that when the tidal water is receding, ebb flow from the shallow intertidal mudflats especially from the northern and western part of Urir Char area causes stronger flow towards the north direction compared to east direction at the measurement location. This explains the stronger northward component of ebb velocity compared to eastward component in Fig. 6. The small rise in observed turbidity values during the peak ebb velocity, as shown in Fig. 6, appears to be due to the smaller magnitude ebb current as well as lesser supply of sediments from horizontal advection. The shorter (less than 1 hour) phase difference between peak ebb current and peak turbidity values can also be understood from this Figure. As the western channel of Urir Char Island shows slack water with very small velocity, very little sediments are transported from this area towards the measurement location B. So, the peak of the turbidity may be only caused by the local pickup of the sediments by tidal currents with a time lag created by hysteresis relationship of resuspension, as discussed by Barua (1990) also in case of Meghna Estuary. Also, simulation results show that during this period slack water appears at the shallow western channel of the Urir Char Island as well as along one of the southern channels (the one at the south-west). As a result, the receding water from the western channel of Urir Char Island is directed towards the east along the southern channel of the island. This creates relatively strong ebb current along the southern part of Urir Char

Island. Also, magnitude of ebb current at this instance along the Sandwip Channel is relatively stronger compared to the previous one (Fig. 8) while it is opposite for the channel at the south of Urir Char Island.

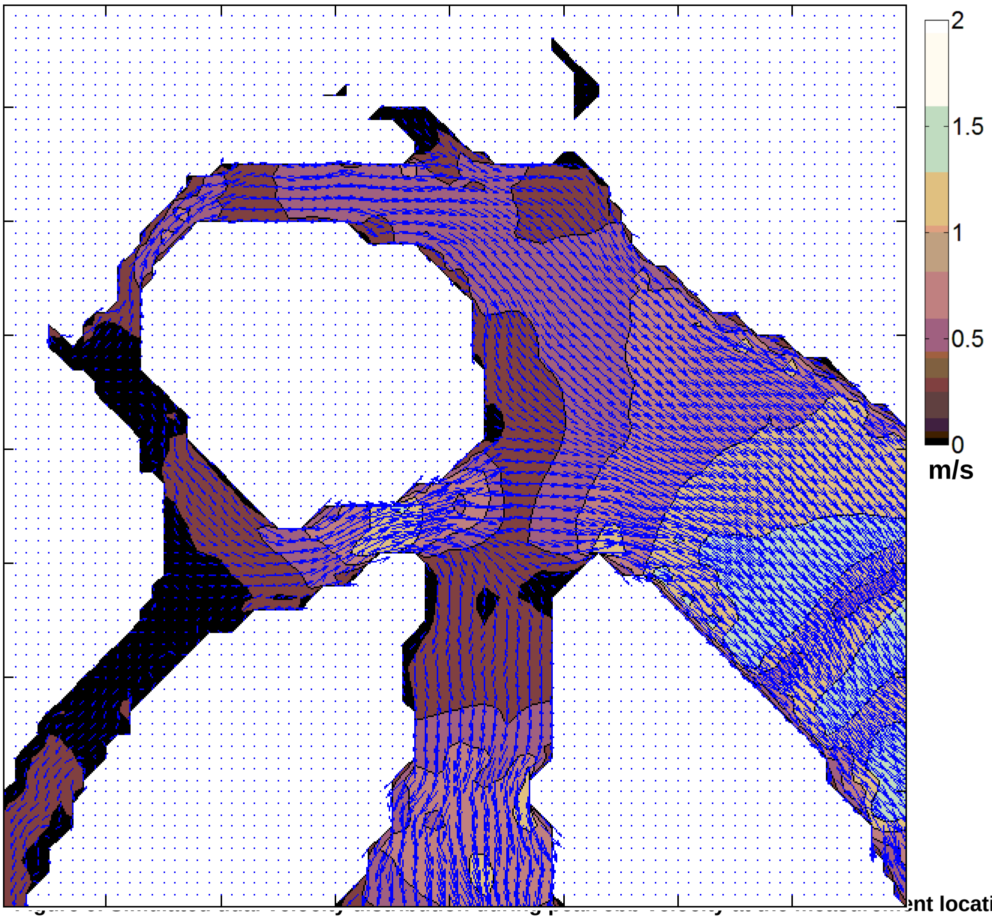

Figure 9. Simulated tidal velocity distribution during peak ebb velocity at the measurement location B, along with contour of velocity magnitude (m/s)

Tidal Current Features

The flood and ebb tidal current features inferred from the observation data and simulation results are summarized in Fig. 10. In this Figure firm arrows show the characteristic flood tidal currents which arrives at the study area primarily from the Sandip Channel at the southeast. This flow inundates the shallow intertidal mudflats of the Urir Char Island from the north and northwestern direction. The steep slope at the Noakhali mainland side contributes to the formation of such flow characteristics. The dotted arrows in Fig. 10 show the characteristic ebb currents. During the ebb period, at first tidal waters recede from the shallow mudflats and flows towards north-west and north direction, resulting strong north-ward current along the northern channel of Urir Char Island. It appears that the mainland Noakhali side encounters strong tidal currents both during flood and ebb periods, which may be the reason behind severe erosion along the coastline of this area. The strong flood velocity along with long duration of slack water during flood periods appears to cause residual transport of coarse and fine sediments towards the intertidal mudflat areas around the Urir Char Island resulting in sedimentation and accretion along the northern, western and eastern parts of this island.

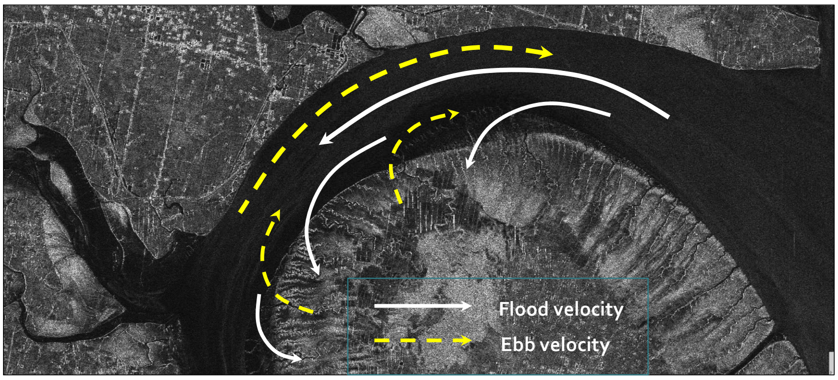

Figure 10. Tidal current features around the study site

CONCLUSIONS

Observed tidal water level, velocity components and turbidity data collected from around Urir Char Island at the north-eastern part of the Meghna Estuary have been explained through a 2DH numerical model. It has been found that strong tidal asymmetry exists at the highly accreting north-eastern part of the Meghna Estuary. Along the northern channel of Urir Char Island flood velocity exceeds ebb velocity which would induce residual transport of coarse sediments towards land. Also slack duration before ebb is shorter than slack duration before flood indicating residual transport of fine sediments. The phase lag between peak flood velocity and peak turbidity during the flood duration is about two hours, while it is less than one hour between peak ebb velocity and peak turbidity during ebb duration. A ‘second peak’ in the turbidity profiles is observed which appears to be caused by the rundown of ebb tidal flow from the shallow intertidal mudflats around the Urir Char Island. From the simulation results, it is evident that the horizontal advection pattern plays significant role in residual transport of suspended sediments.

ACKNOWLEDGMENTS

This research work has been carried out under a collaborative project titled ‘Investigation of sedimentation process and stability of the area around the cross-dams in the Meghna Estuary’ supported by Space Application for Environment (SAFE), one of international activities under the Asia-Pacific Regional Space Agency Forum (APRSAF). It has been financially and technically supported by Japan Aerospace Exploration Agency (JAXA).

REFERENCES

Azam, M. H., Jakobsen, F., Kabir, M. U. & Hye, J. M. A. 2000. Sensitivity of the tidal signal around Meghna Estuary to the changes in river discharge: a model study. *Proceedings of the Twelfth Congress of the Asia and Pacific Division of the International Association for Hydraulic Engineering and Research* (Bangkok, Thailand), 375–384.

Barua, D.K. 1990. Suspended sediment movement in the estuary of the Ganges-Brahmaputra-Meghna river system. *Marine Geology*, 91: 243-253.

Coleman, J.M. 1969. Brahmaputra River: Channel processes and sedimentation, *Sediment Geol.*, 3 (1969), pp.129-239.

de Wilde, K. (ed.) 2011. *Moving Coastlines: Emergence and Use of Land in the Ganges-Brahmaputra-Meghna Estuary*. University Press Limited, Dhaka.

Dronkers, J. 1986. Tidal asymmetry and estuarine morphology. *Netherlands Journal of Sea Research*, 20(2/3), 117 – 131.

Hussain, M. A., Tajima, Y., Taguchi, Y. and Gunasekara, K. 2013. Tidal Characteristics Affected by Dynamic Morphology Change in the Meghna Estuary, *Proceedings of the 7th International Conference on Asian and Pacific Coasts* (APAC), September 24-26, Bali, Indonesia.

Hussain, M.A., Tajima, Y., Gunasekara, K., Rana, S. and Hasan, R. 2014. Recent coastline changes at the eastern part of the Meghna Estuary using PALSAR and Landsat images, *Proceedings of the 7th IGRSM International Conference and Exhibition on Remote Sensing and GIS*, Kuala Lumpur, Malaysia, 21-22 April. IOP Conf. Series: Earth and Environmental Science 20, 012047 doi:10.1088/1755-1315/20/1/012047.

Hussain, M. A. and Tajima, Y. 2014. Tidal Propagation Characteristics at the Eastern Part of Meghna Estuary. *Journal of Coastal Research* (in submission).

Islam, M. R., Begum, S. F., Yamaguchi, Y. and Ogawa, K. 2002. Distribution of suspended sediment in the coastal sea off the Ganges-Brahmaputra River mouth: observation from TM data, *Journal of Marine Systems*, 32, 307-321.

Matsumoto, K., Takanezawa, T. and Ooe, M. 2000. Ocean Tide Models Developed by Assimilating TOPEX/POSEIDON Altimeter Data into Hydrodynamical Model: A Global Model and a Regional Model Around Japan, *Journal of Oceanography*, 56, 567-581.

Milliman, J.D. 1991. Flux and fate of fluvial sediment and water in coastal seas. In: Mantoura, R.F.C., Martin, J.-M. & Wollast, R. (eds). *Ocean Margin Processes in Global Change*. John Willey and Sons Ltd., Chichester, 69-89.

Wang, Z. B., Jeuken, C. and de Vriend, H.J. 1999. *Tidal asymmetry and residual sediment transport in estuaries*, WL | delft hydraulics.